Metallomics

RSC Publishing

PAPER

View Article Online
View Journal | View Issue

Cite this: *Metallomics*, 2013, **5**, 855

Chemical interactions of mercury species and some transition and noble metals towards metallothionein (Zn_7MT-2) evaluated using SEC/ICP-MS, RP-HPLC/ESI-MS and MALDI-TOF-MS†

Ming Xu,[a] Limin Yang[a] and Qiuquan Wang*[ab]

Received 14th January 2013,
Accepted 13th March 2013

DOI: 10.1039/c3mt00016h

www.rsc.org/metallomics

The chemical affinities of three submetallomes (''Mn, Co, Ni, Cu, Cd''; ''Pd, Pt, Au''; and ''Hg, CH_3Hg, C_2H_5Hg-THI'') towards metallothionein-2 (Zn_7MT-2) in a physiological solution environment were evaluated using SEC/ICP-MS together with RP-HPLC/ESI-IT-MS and MALDI-TOF-MS, and followed the order: ''Zn^{2+} < Cu^{2+}, Cd^{2+} > Ni^{2+} > Mn^{2+}, Co^{2+}''; ''Pd^{2+} > Au^{3+} > Pt^{2+}''; and ''Hg^{2+} > CH_3Hg^+ > C_2H_5Hg-THI''. Besides these, the structural change and composition of the CH_3Hg–MT-2 complexes formed during the CH_3Hg^+ titration process were further investigated using CD spectroscopy, RP-HPLC/ESI-MS and MALDI-TOF-MS, indicating that linear and more hydrophobic $(CH_3Hg)_x$MT-2 (x = 12, 13, 14, 15, 16, 17, 18, 19 and 20) were formed. This information is important in understanding the interactions of the metals with Zn_7MT-2 and their corresponding biological functions and toxicities.

Introduction

Most of the elements in the periodic table of the elements can be found in significant to trace amounts existing as free ions and/or associated with biomolecules in organisms, regardless of their beneficial and/or harmful effects. As some of the most important biomolecules, metalloproteins play a vital role and are a key to understand biological processes. More than one third of proteins are metalloproteins, and more proteins are involved with metals or metalloids for their function.[1] The degree of metal binding in a protein molecule depends on its stereostructure domain site, which is composed of selective chemical functional groups of the protein side chains. Theoretically, these stereostructure domain sites can show different chemical affinities to various metal ions, and this difference allows metalloproteins to serve in the storage of metal ions (sometimes for detoxification) and/or as transporters of them, and in turn the metal ions help the metalloprotein to accomplish its functions. Research on the binding properties of a metal towards a protein always provides direct insight into the molecular mechanisms of the functions of both the metal and the protein. This kind of research mostly lies in the newly emerging research field of metallomics.[2]

Metallothioneins (MTs) are a super family of cysteine-rich and low molecular weight proteins. They were discovered over 50 years ago and have been identified in bacteria, fungi, algae, plants, crustaceans and fishes to mammals, exhibiting an obvious evolutionary relationship.[3–5] The expression of MTs in organisms is generally considered as a biomarker for detoxification in response to heavy metals, free radicals and oxidative agents. For mammals, the MTs consist of, in general, approximately 60 amino acid residues, and contain two metal-binding domains: the α domain (eleven cysteine residues) and the β domain (nine cysteine residues). There are no disulfides, aromatic amino acids or histidine in the molecules. The extraordinary reactivity of the sulfhydryl group (–SH) in cysteine residues allows MTs to be involved in the regulation of physiological metals (*e.g.* Zn) and provides protection against other adventitious toxic metals and their corresponding species. Toxic metals may replace the Zn in the MTs, and induce the formation of more MTs for the deactivation of the toxic metals.[6]

The binding properties of MTs to metal/metalloid elements such as Zn, Cd, Cu, Hg, Bi and As have been studied, focusing on the metalation and demetalation of MTs based on the use of UV-vis absorption and circular dichroism (CD) spectroscopies as well as electrospray ionization mass spectrometry (ESI-MS). These optical spectroscopic and ESI-MS studies have provided

[a] *Department of Chemistry & the Key Laboratory of Analytical Sciences, College of Chemistry and Chemical Engineering, Xiamen University, Xiamen 361005, China. E-mail: qqwang@xmu.edu.cn; Fax: +86 592 2187400; Tel: +86 592 2181796*

[b] *State Key Laboratory of Marine Environmental Science, Xiamen University, Xiamen 361005, China*

† Electronic supplementary information (ESI) available: Operating conditions of ICP-MS, ESI-IT-MS and MALDI-TOF-MS, ESI-MS spectra of Zn_7MT-2 and SEC/ICP-MS chromatograms of Zn_7MT-2 reacting with metal ions. See DOI: 10.1039/c3mt00016h

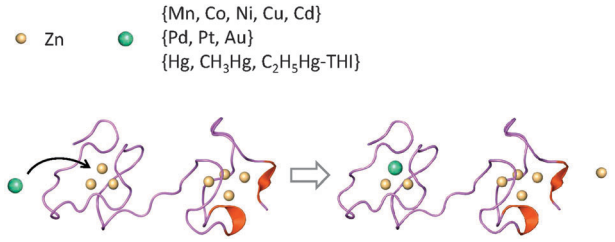

Fig. 1 The chemical structure of Zn_7MT-2 and the three submetallomes studied.

information on binding site geometric changes as a function of metal loading and/or structural changes that occurred in the MTs themselves induced by metalation.[7] In this study, an element-specific detection technique (inductively coupled plasma mass spectrometry, ICP-MS) coupled with a gentle separation technique (size-exclusion chromatography, SEC) together with RP-HPLC/ESI-MS and MALDI-TOF-MS as well as CD spectroscopy, which provide information on chemical composition and structural changes of MTs,[7–10] were used to study the chemical interactions of some metallic species with a typical MT, Zn_7MT-2 (Zn-induced from rabbit liver). The unique features of ICP-MS, for example, multi-element determination ability with high selectivity and sensitivity, allowed us to perform a high-throughput evaluation of the interaction between Zn_7MT-2 and metallic species in a physiological solution environment. The chemical affinity and binding process of three submetallomes ["Mn, Co, Ni, Cu, Cd"; "Pd, Pt, Au"; and especially "Hg, methylmercury (CH_3Hg) and thimerosal (C_2H_5Hg-THI)"] towards Zn_7MT-2 (Fig. 1) were evaluated in this study.

Experimental

Reagents

Zn_7MT-2 (>90%, from rabbit liver) was purchased from Hunan Lugu Biotechnology Co., Ltd. China, as a dry powder stored at −20 °C, and its solution (0.76 mmol L^{-1}) was freshly prepared before each experiment with buffer solution (10 mM Tris-HCl, pH 7.4). Methylmercuric chloride (CH_3HgCl, 98.5%) obtained from Dr Ehrenstorfer GmbH, Germany, and ethylmercurithiosalicylate (C_2H_5Hg-THI, 98%) from Shanghai Sangon Biological Engineering Technology and Service Co., Ltd. China, were used to prepare their stock solutions (1000 μg mL^{-1}). Stock Hg solution (1007 μg mL^{-1} in 9.2% HNO_3) was purchased from Sigma-Aldrich (Saint Louis, Missouri). The standard solutions of Mn, Co, Ni, Cu, Cd, Pd, Pt and Au were all prepared by dissolving their inorganic chlorides (>98%) in nitric acid (GR grade, 65%, Merck, Darmstadt, Germany). All of these standard solutions (1000 μg mL^{-1} in 2% HNO_3) were stored in Teflon bottles before use. Other reagents used were at least of analytical-reagent or higher available purity grade. Ultra-pure water (18.2 MΩ cm, Pen-Tung Sah Micro-Electro-Mechanical Systems Research Center of Xiamen University, China) degassed by nitrogen gas was used throughout this study.

Instrumentation

Elemental analysis was performed on an ELAN DRC II ICP-MS (PerkinElmer, SCIEX, Canada), in which DRC stands for dynamic reaction cell. The ICP-MS was equipped with an integral peristaltic pump, a concentric pneumatic nebulizer, and a cyclonic spray chamber. O_2 (99.999%) used as a reaction gas was purchased from Beijing AP Beifen Gases Industry Co. (Beijing, China). Sulfur determination was achieved by introducing O_2 into the DRC to form $^{32}S^{16}O^+$ instead of monitoring $^{32}S^+$, thus eliminating the strong spectral interferences such as $^{16}O_2^+$. Chromatographic separation of the free metal ions and their complexes with MT-2 was carried out on a SERIES 200 HPLC system (PerkinElmer, SCIEX, Canada) equipped with an autosampler, a vacuum degasser and a 200 μL sample loop as well as a size exclusion column (Superdex 75 10/300 GL, 300 × 10 mm I.D., 13 μm, GE Healthcare, Uppsala, Sweden). The chromatographic effluent was directly infused into the ICP-MS after the SEC separation with a mobile phase containing 5 mM Tris and 100 mM NH_4HCO_3 (pH 7.4) with a flow rate of 0.75 mL min^{-1}.

For RP-HPLC/ESI-IT-MS analysis, an Agilent 1100 series chromatographic system (Agilent Technologies, Palo Alto, CA, USA) was coupled with an Esquire-LC ESI ion trap mass spectrometer (ESI-IT-MS, Bruker Daltonics, Bremen, Germany). A VP-ODS C18 column (250 × 2.0 mm I.D., 5 μm, Shimadzu, Japan) was used for separation, and a gradient elution program was set to linearly increase the percentage of mobile phase B (acetonitrile) from 5% to 80% with a flow rate of 0.15 mL min^{-1} (mobile phase A: ultra-pure water). MALDI-TOF-MS experiments were performed with a Bruker microflex LRF matrix assisted laser desorption and ionization time-of-flight mass spectrometer (Bruker Daltonics, Bremen, Germany). The mass calibrations of MALDI-TOF-MS were the average of at least 100 shots with the software provided by the manufacturer using a Peptide and Protein MALDI-MS Calibration Kit (700 to 66 000 Da, Sigma-Aldrich). Detailed instrumental setting parameters for the ICP-MS, ESI-IT-MS and MALDI-TOF-MS systems are listed in Table S1 (ESI†). The data obtained from these three instruments were analyzed using the software stations provided by their manufacturers.

CD spectra were acquired on a J-810 spectropolarimeter (Jasco, Japan) using a 1 mm path length quartz cell for the near- and far-UV range measurements at room temperature. The data were collected from 190 to 350 nm using a response time of 1 s and a scan speed of 100 nm min^{-1}. Spectra represent an average of five scans with the background corrected against a buffer blank.

Experimental procedures

Analysis of the binding affinities of different metal ions towards Zn_7MT-2. Before use, the Zn_7MT-2 standard was firstly analyzed using SEC/ICP-MS and RP-HPLC/ESI-IT-MS to characterize its chemical composition. For SEC/ICP-MS analysis, the isotopes of ^{63}Cu, ^{66}Zn, ^{111}Cd and $^{32}S^{16}O$ were monitored during analysis. For RP-HPLC/ESI-IT-MS, the RP-HPLC separation was operated at three pH conditions (pH 3, 5 and 6) by adjusting the mobile phase with diluted acetic acid and ammonia solutions. The ESI-IT-MS was set to the positive mode with a scan range from 50 to 2000 Da.

All chemical reactions were carried out in a buffer solution (10 mM Tris-HCl, pH 7.4) at 25 °C. For measurements at

different molar ratios of the metal ion to Zn_7MT-2, calculated volumes of each element standard solutions ("Mn, Co, Ni, Cu, Cd" or "Pd, Pt, Au") were mixed together and then added into Zn_7MT-2 solution. After incubation for 1 h at 25 °C, the samples were analyzed with SEC/ICP-MS. Between each analysis, the SEC column was eluted with 10 mM EDTA to clean away excess free metal ions trapped on the column, and then equilibrated with the mobile phase. The isotopes of ^{55}Mn, ^{59}Co, ^{60}Ni, ^{63}Cu, ^{66}Zn, ^{111}Cd, ^{106}Pd, ^{195}Pt, ^{197}Au and $^{32}S^{16}O$ were monitored using ICP-MS.

The binding properties of Hg species towards Zn_7MT-2. Again, calculated volumes of Hg species (Hg^{2+}, CH_3Hg^+ and C_2H_5Hg-THI) were respectively titrated into Zn_7MT-2 solution buffered by 10 mM Tris-HCl (pH 7.4) to obtain different molar ratios (1, 2, 3, 4, 6, 8, 10, 20, 40, 60, 80 and 100). After incubation for 1 h at 25 °C, the samples were analyzed with SEC/ICP-MS, and ^{66}Zn, ^{202}Hg and $^{32}S^{16}O$ were monitored. Between each analysis, the SEC column was eluted with 10 mM EDTA and 0.05% (*v*/*v*) 2-mercaptoethanol to clean away the replaced Zn^{2+} and excess Hg species, and then equilibrated with the mobile phase.

For structure analysis, a known volume of CH_3Hg^+ solution was titrated into a 15 μmol L^{-1} Zn_7MT-2 solution (10 mM Tris-HCl, pH 7.4) at room temperature. Through continuous addition of CH_3Hg^+, the CD spectra were scanned at different molar ratios of CH_3Hg^+ to Zn_7MT-2 ($n_{CH_3Hg^+}/n_{MT\text{-}2}$ = 0, 6, 10, 20, 40 and 100). For RP-HPLC/ESI-IT-MS analysis, 20 μL Zn_7MT-2 sample titrated with CH_3Hg^+ at the molar ratio of $n_{CH_3Hg^+}/n_{MT\text{-}2}$ = 20 was injected into the column (pH 3). Meanwhile, the same sample was crystallized with sinapinic acid solution for MALDI-TOF-MS analysis.

Safety note: *mercury species are toxic, and physical exposure to them during the experimental process should be very carefully avoided*!

Results and discussion

Analysis of Zn_7MT-2 with SEC/ICP-MS and RP-HPLC/ESI-IT-MS

In *Homo sapiens*, there are four kinds of MTs, namely MT-1, MT-2, MT-3 and MT-4. The most widely expressed MTs in the human body are MT-1 and MT-2, while MT-3 and MT-4 are mainly expressed in the central nervous system and stratified squamous epithelia, respectively.[6] Due to the availability of its commercial products, we selected Zn_7MT-2 from rabbit liver as a model in this study, which has a similar amino acid sequence and the same 20 cysteine residues as that of humans.

Zn_7MT-2 was analyzed using SEC/ICP-MS, and four isotopes (^{63}Cu, ^{66}Zn, ^{111}Cd and $^{32}S^{16}O$) were monitored (Fig. 2). As expected, this MT-2 standard mainly existed as its Zn form (>92%), and in the chromatogram there are two peaks at elution times of 15.2–17.0 and 17.0–19.8 min. The first and second peaks should correspond to the dimer and/or trimer and monomer of Zn_7MT-2, respectively.[11] The same sample was analyzed in parallel using RP-HPLC/ESI-IT-MS under three pH conditions (pH 3, 5 and 6). At these pH values (Fig. S1, ESI†), the molecular weights of the most abundant MT-2 subisoform (N Ac-MT-2a) were calculated to be 6124.3, 6314.9 and 6569.5 Da,

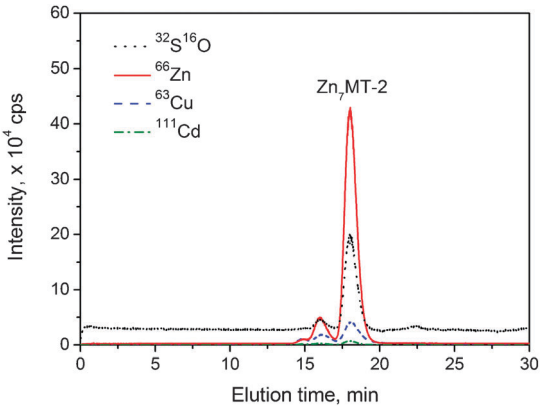

Fig. 2 Chromatograms of the Zn_7MT-2 standard analyzed by SEC/ICP-MS at pH 7.4.

corresponding to apo-MT-2, Zn_3MT-2 and Zn_7MT-2, respectively. In Fig. S1d (ESI†), peaks belonging to subisoforms of rabbit liver MT-2 can be observed at masses of 870.2 (MT-2a), 874.4 (MT-2c), 876.0 (N Ac-MT-2a), 879.0 (N Ac-MT-2b), 880.3 (N Ac-MT-2c) and 892.5 (N Ac-MT-2e) Da in the mass range of 850–900 Da.[12] Other subisoforms could not be characterized by the ESI-IT-MS used in this study because of its limited resolution and sensitivity. It should be noted that the ionization efficiency of the Zn_7MT-2 molecule was seriously affected by pH. When the pH approached near neutral, the total ion signal of MT-2 was remarkably decreased, and the background in Fig. S1b and c (ESI†) became complicated due to interference signals. Besides the pH conditions, organic solvent as well as the degree of Zn-metalation of the MT-2 also influenced the MS signals significantly. We thus switched to SEC/ICP-MS to study the interactions between metals and Zn_7MT-2 under physiological solution conditions (pH 7.4).

Zinc exchange in Zn_7MT-2 by the typical transition and noble submetallomes evaluated using SEC/ICP-MS

In the toxicity response process, metal substitution in MT molecules acts as a mechanism of MT-mediated metal detoxification.[13] The Zn^{2+} in a MT may be replaced by the metal ion which has the stronger affinity towards the MT, and, in turn, induce the synthesis of more MTs for deactivation of the metal.[6] In order to compare the interactions between different metals and Zn_7MT-2, the signals of S, Zn and the adventitious metals were monitored simultaneously using SEC/ICP-MS. As a naturally occurring element in MT-2 molecules, the number of S atoms (20 in cysteine and 1 in methionine residues, UniProt: P18055) is genetically fixed and can be used to represent the MT-2 content. We could thus monitor the metal ion substitution processes of Zn^{2+} in Zn_7MT-2 through the ICP-MS intensity ratio of the metal to S (I_M/I_{SO}) in the metal–MT-2 complexes formed, while the replaced Zn^{2+} and the excess metal ions were trapped on the SEC.

To validate the reliability of SEC/ICP-MS, the submetallome selected included five typical transition metals (Mn, Co, Ni, Cu and Cd) that are essential trace elements, except Cd. From the viewpoint of bioinorganic coordination chemistry, all these metal ions can form metal–thiolate bonds with the –SHs in

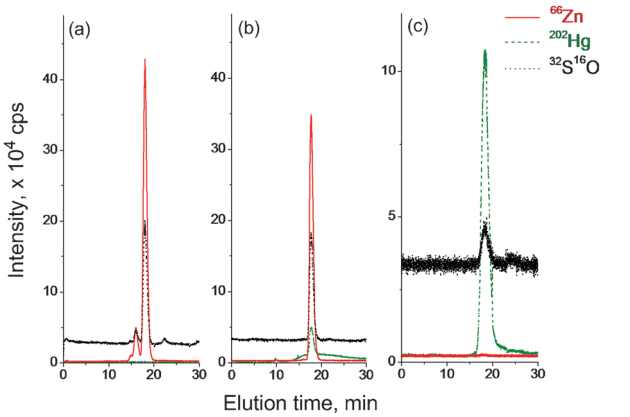

Fig. 3 SEC/ICP-MS chromatograms of Zn_7MT-2 (a), reacting with CH_3Hg^+ at $n_{CH_3Hg^+}/n_{MT\text{-}2}$ = 1 (b) and 100 (c) at pH 7.4.

apo-MT-2 molecules *in vitro*. When the MT-2 exists as the Zn_7MT-2 form, obvious replacement of Zn^{2+} was observed only in the case of Cu^{2+} and Cd^{2+} but not for Mn^{2+}, Co^{2+} and Ni^{2+} (Fig. S2a and b, ESI†). By increasing the molar ratio of the metal to Zn_7MT-2 ($n_M/n_{MT\text{-}2}$), Cu^{2+} and Cd^{2+} could progressively replace more Zn^{2+} in Zn_7MT-2 molecules. For Ni^{2+}, this substitution only happened when the molar ratio exceeded one hundred, indicating that the Zn_7MT-2 is relatively thermodynamically stable in a high Ni^{2+} environment. No obvious change was observed in the case of Mn^{2+} and/or Co^{2+} under our experimental conditions. The chemical affinities of the metals (Mn, Co, Ni, Cu, Zn and Cd) to the MT-2 could be thus concluded as $Zn^{2+} < Cu^{2+}$, $Cd^{2+} > Ni^{2+} > Mn^{2+}$, Co^{2+}. These results are in accordance with the Irving–Williams series for divalent metals which is essentially independent of the ligand,[14] suggesting that SEC/ICP-MS is effective for evaluating the chemical affinities of different metals towards Zn_7MT-2.

Noble metals such as Pd, Pt and Au selected in this study are not in high abundance in ecosystems or organisms, but their organometallic and/or inorganic compounds are very often used as anticancer agents, imaging sensors and industrial catalysts.[15,16] These kinds of artificial chemicals bring potential environmental and health hazards, and therefore have become an increasing focus of attention.[17,18] Fig. S2c and d (ESI†) show that Zn^{2+} was replaced remarkably along with an increase in the molar ratios of Pd^{2+}, Au^{3+} and Pt^{2+} to Zn_7MT-2. The strong chemical affinity between these metal ions (Pd^{2+}, Au^{3+} and Pt^{2+}) and −SHs allowed the replacement of Zn^{2+} in Zn_7MT-2. Based on these results, Pd^{2+} seemed to have a stronger affinity than Au^{3+} and Pt^{2+} to Zn_7MT-2. However, it should be pointed out that these metals are used in the forms of organometallic complexes in most cases, and their reactivities with Zn_7MT-2 could differ from those free metal ions, and therefore their biological implications need to be further investigated.

Chemical affinity of Hg species towards Zn_7MT-2

Hg vapor from amalgam tooth fillings, CH_3Hg^+ in fish and $C_2H_5Hg^+$ in the form of C_2H_5Hg-THI are three of the means of Hg exposure for billions of people.[19] It has already been found that MTs are important protective factors against the toxicity of Hg.[20,21] For MT-2, it can bind with Hg^{2+} to form Hg_7–MT (tetrahedral coordination geometry), Hg_{12}–MT (trigonal) and Hg_{18}–MT (linear) complexes under *in vitro* conditions,[22] which provides strong evidence for its use in detoxification *in vivo*.[23] For CH_3Hg^+ and C_2H_5Hg-THI, although there are some studies focusing on their relationship with MTs or Zn^{2+} *in vivo*,[24,25] fundamental *in vitro* information is limited.

Taking CH_3Hg^+ as an example, the SEC/ICP-MS results show that it could gradually replace all the Zn^{2+} in Zn_7MT-2 along with an increase in the molar ratio (Fig. 3). Besides this, CH_3Hg^+ binding with –SHs destroyed the stereostructure of the α- and β-domains of the Zn_7MT-2 to form unordered linear $(CH_3Hg)_x$MT-2 complexes as indicated by CD spectroscopic studies (Fig. 4) because CH_3Hg^+ bound with –SH in a quasi-covalent way, and the existence of a methyl group made the complexes more hydrophobic, thus decreasing its solubility in the physiological solution and causing the degressive $^{32}S^{16}O$ intensity shown in Fig. 3b and c. This provided evidence for the toxicity of CH_3Hg^+ as it could denature the native protein molecule.

In order to further study the structural changes of MT-2 caused by CH_3Hg^+, the conformation change of the MT-2 complex during the interaction process was studied using CD spectroscopy (Fig. 4). Based on the available structural information in the PDB database (PDB 1MRB and PDB 2MRB), the secondary structure of Zn_7MT-2 has the same molecular architecture as Cd_7MT-2 containing several half-turns and 3_{10}-helix segments as well as a random coil.[26] The CD curve of Zn_7MT-2 in Fig. 4 was characterized by (1) a minimum centered at 200 nm, (2) a weak negative shoulder between 220 and 230 nm, and (3) a positive band at 244 nm, which should correspond to the random coil (1), 3_{10}-helix (2) and Zn–thiolate cluster (3), respectively.[27,28] After the addition of CH_3Hg^+, the gradual disappearance observed of this characteristic CD fingerprint of Zn_7MT-2 indicated new unordered structures were formed as the Zn^{2+} in the Zn_7MT-2 was replaced by CH_3Hg^+ and interaction developed between the MT-2 and CH_3Hg^+.

Moreover, the compositions of $(CH_3Hg)_x$MT-2 complexes formed at $n_{CH_3Hg^+}/n_{MT\text{-}2}$ = 20 were characterized using MALDI-TOF-MS

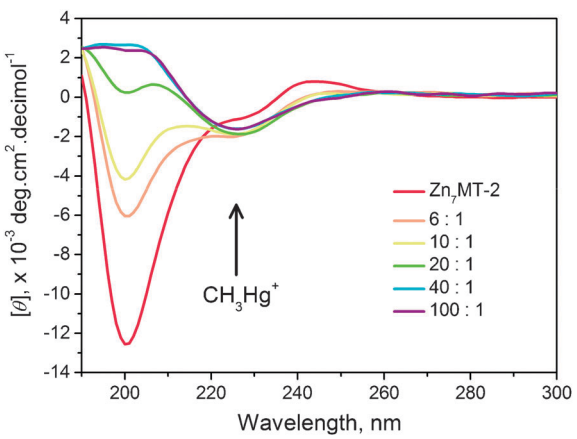

Fig. 4 Titration CD spectra of Zn_7MT-2 with CH_3Hg^+ at pH 7.4.

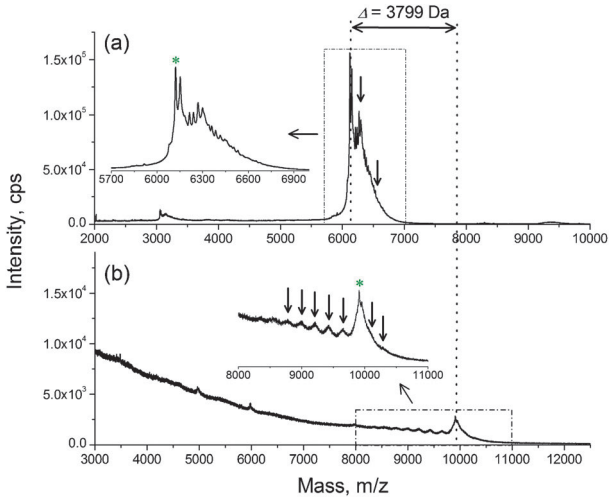

Fig. 5 MALDI-TOF-MS of Zn_7MT-2 (a) and CH_3Hg–MT-2 complexes (b) formed after the titration with CH_3Hg^+ at $n_{CH_3Hg^+}/n_{MT\text{-}2}$ = 20.

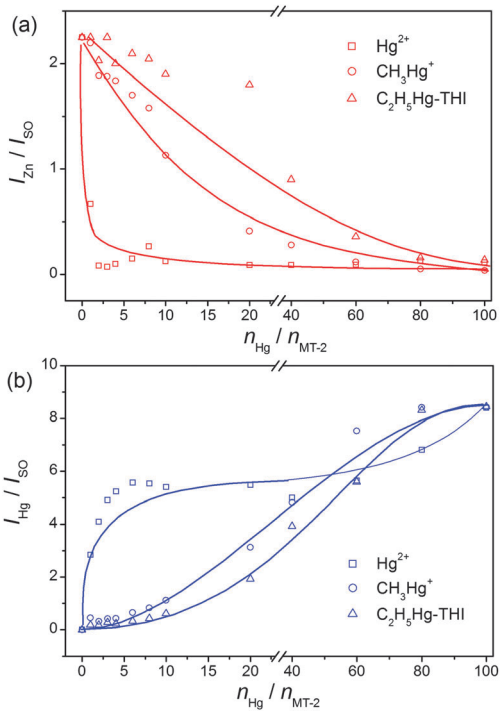

Fig. 7 Substitution of the Zn^{2+} in Zn_7MT-2 by Hg^{2+}, CH_3Hg^+ and C_2H_5Hg-THI (a) and the binding process of the three Hg species with MT-2 (b) at different molar ratios ($n_{Hg}/n_{MT\text{-}2}$) at pH 7.4.

and RP-HPLC/ESI-IT-MS. Because sinapinic acid (pH < 6) was used as a matrix in the MALDI-TOF-MS, the Zn_7MT-2 was detected mainly as the apo-MT-2 form (* peak in Fig. 5a, 6124.5 Da) although some Zn_3MT-2 (6312.1 Da) and Zn_7MT-2 (6567.1 Da) could also be observed at the tip positions of the arrows. In the enlarged figure of Fig. 5a, other subisoforms of MT-2 could also be observed which was in accordance with the RP-HPLC/ESI-IT-MS results (Fig. S1d, ESI†). The $(CH_3Hg)_x$MT-2 complex (* peak in Fig. 5b) detected is 3799 Da heavier than the apo-MT-2. The value of x was calculated to be between 17 and 18, suggesting that $(CH_3Hg)_{17}$MT-2 and $(CH_3Hg)_{18}$MT-2 are the dominant forms under these experimental conditions, which is in accordance with the results obtained using RP-HPLC/ESI-IT-MS (Fig. 6). Other $(CH_3Hg)_x$MT-2 complexes (x = 12, 13, 14, 15, 16, 19 and 20) could also be found in much lower abundance in the same medium (arrow positions in Fig. 5b). As shown in Fig. 6, $(CH_3Hg)_{17}$MT-2 and $(CH_3Hg)_{18}$MT-2 as well as $(CH_3Hg)_{19}$MT-2 and $(CH_3Hg)_{20}$MT-2 could be clearly observed, suggesting their formation. Under the physiological solution environment conditions (pH 7.4) in this study, continual titration ($n_{CH_3Hg^+}/n_{MT\text{-}2}$ > 20) enforced the formation of higher stoichiometric ratio $(CH_3Hg)_x$MT-2 complexes (x > 18) until a reaction equilibrium was reached. This is the first report of mass spectroscopic studies on the interactions of CH_3Hg^+ with Zn_7MT-2.

Based on the measured I_{Hg}/I_{SO} and I_{Zn}/I_{SO} values, the binding processes of Hg^{2+}, CH_3Hg^+ and C_2H_5Hg-THI with Zn_7MT-2 were compared. Fig. 7a and b show that Zn^{2+} was continually released from the Zn_7MT-2 molecule as the molar ratio increased until all the −SHs were occupied by Hg^{2+}, CH_3Hg^+ and the $C_2H_5Hg^+$ from C_2H_5Hg-THI. Compared with CH_3Hg^+ and C_2H_5Hg-THI that could form R–Hg–S– (R = CH_3Hg^+ or $C_2H_5Hg^+$) with –SH,[29] Hg^{2+} formed –S–Hg–S– bonds besides –Hg–S– with –SHs, resulting in a much faster replacement of Zn^{2+}, and exhibited the strongest affinity towards MT-2 among the three Hg species.

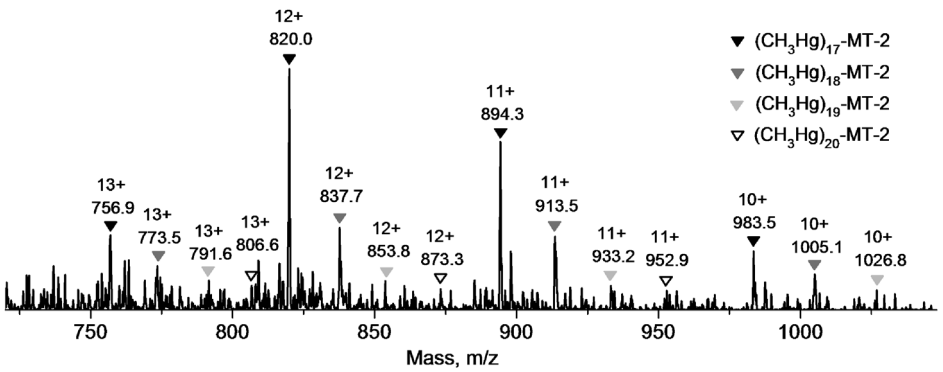

Fig. 6 RP-HPLC/ESI-IT-MS of CH_3Hg–MT-2 complexes formed after the titration of Zn_7MT-2 with CH_3Hg^+ at $n_{CH_3Hg^+}/n_{MT\text{-}2}$ = 20.

Compared with CH_3Hg^+, the $C_2H_5Hg^+$ in C_2H_5Hg-THI had to be released first before attacking the –SH in Zn_7MT-2, leading to its binding process with the MT-2 being much slower than that of CH_3Hg^+. The $C_2H_5Hg^+$ cannot be released from the C_2H_5Hg-THI molecule until it approaches another –SH.[30] This is why C_2H_5Hg-THI has been used in vaccines as a preservative for many years, and it is less toxic and much safer than the direct use of CH_3Hg^+ or $C_2H_5Hg^+$. Similar phenomena whereby intracellular Zn^{2+} concentration increases after exposure to CH_3Hg^+ and/or C_2H_5Hg-THI have been observed when studying the toxicity of CH_3Hg^+ and/or C_2H_5Hg-THI *in vivo*.[31,32] Thus, it can be concluded that the binding affinities of these Hg species towards Zn_7MT-2 is in the order $Hg^{2+} > CH_3Hg^+ > C_2H_5Hg$-THI.

Conclusions

The chemical affinities and Zn-exchange abilities of three submetallomes towards Zn_7MT-2 were evaluated using SEC/ICP-MS, in which the S in Zn_7MT-2 could serve as a natural internal standard. The binding properties and processes of Zn_7MT-2 to the metallic species in the submetallomes could be observed in a physiological solution environment. More importantly, the interaction of CH_3Hg^+ with the MT-2 was further evaluated using MALDI-TOF-MS and RP-HPLC/ESI-IT-MS as well as CD spectroscopy, offering valuable information on the composition and stereostructural change of the CH_3Hg–MT-2 complexes. The information obtained is helpful in understanding the biological functions of metals (especially Hg species) and metallothioneins. Moreover, it should be expected that SEC/ICP-MS together with molecular mass spectrometry could be applied to *in vivo* studies of the roles of metals and interactions between the metals and metalloproteins (not limited to Zn_7MT-2) during certain biological life processes in the near future.

Acknowledgements

This study was financially supported by grants from the National Natural Science Foundation of China (No. 21035006 and 21275120) and the National Basic Research Program 973 Project (No. 2009CB421605). We thank Prof. John Hodgkiss of The University of Hong Kong for his assistance with English.

References

1 J. A. Tainer, V. A. Roberts and E. D. Getzoff, *Curr. Opin. Biotechnol.*, 1991, **2**, 582–591.
2 R. Lobinski, J. S. Becker, H. Haraguchi and B. Sarkar, *Pure Appl. Chem.*, 2010, **82**, 493–504.
3 M. J. Stillman, *Coord. Chem. Rev.*, 1995, **144**, 461–511.
4 P. Coyle, J. C. Philcox, L. C. Carey and A. M. Rofe, *Cell. Mol. Life Sci.*, 2002, **59**, 627–647.
5 J. Chan, Z. Huang, M. E. Merrifield, M. T. Salgado and M. J. Stillman, *Coord. Chem. Rev.*, 2002, **233–234**, 319–339.
6 A. K. West, J. Hidalgo, D. Eddins, E. D. Levin and M. Aschner, *NeuroToxicology*, 2008, **29**, 489–503.
7 T. T. Ngu and M. J. Stillman, *Dalton Trans.*, 2009, 5425–5433.
8 X. Yu, M. Wojciechowski and C. Fenselau, *Anal. Chem.*, 1993, **65**, 1355–1359.
9 K. A. High, B. A. Methven, J. W. McLaren, K. W. M. Siu, J. Wang, J. F. Klaverkamp and J. S. Blais, *Fresenius' J. Anal. Chem.*, 1995, **351**, 393–402.
10 H. Chassaigne and R. Lobinski, *Anal. Chem.*, 1998, **70**, 2536–2543.
11 D. Banerjee, S. Ono and M. G. Cherian, *Toxicology*, 1982, **24**, 95–105.
12 S. Mounicou, L. Ouerdane, B. L'Azou, I. Passagne, C. Ohayon-Courtès, J. Szpunar and R. Lobinski, *Anal. Chem.*, 2010, **82**, 6947–6957.
13 G. Roesijadi, *Cell. Mol. Biol.*, 2000, **46**, 393–405.
14 H. Irving and R. J. P. Williams, *J. Chem. Soc.*, 1953, 3192–3210.
15 K. H. Thompson and C. Orvig, *Science*, 2003, **300**, 936–939.
16 M. Baker, *Nat. Methods*, 2010, **7**, 957–961.
17 A. Casini, A. Karotki, C. Gabbiani, F. Rugi, M. Vašák, L. Messori and P. J. Dyson, *Metallomics*, 2009, **1**, 434–441.
18 D. Hagrman, J. Goodisman, J. C. Dabrowiak and A. K. Souid, *Drug Metab. Dispos.*, 2003, **31**, 916–923.
19 T. W. Clarkson, *Environ. Health Perspect.*, 2002, **110**, 11–23.
20 M. Satoh, N. Nishimura, Y. Kanayama, A. Naganuma, T. Suzuki and C. Tohyama, *J. Pharmacol. Exp. Ther.*, 1997, **283**, 1529–1533.
21 Z. Y. Huang, J. C. Shen, Z. X. Zhuang, X. R. Wang and F. S. C. Lee, *Appl. Organomet. Chem.*, 2004, **18**, 255–261.
22 W. Lu, A. J. Zelazowski and M. J. Stillman, *Inorg. Chem.*, 1993, **32**, 919–926.
23 Z. Pedrero, L. Ouerdane, S. Mounicou, R. Lobinski, M. Monperrusa and D. Amouroux, *Metallomics*, 2012, **4**, 473–479.
24 M. Yoshida, N. Shimizu, M. Suzuki, C. Watanabe, M. Satoh, K. Mori and A. Yasutake, *Environ. Health Perspect.*, 2008, **116**, 746–751.
25 T. Minami, E. Miyata, Y. Sakamoto, H. Yamazaki and S. Ichida, *Cell Biol. Toxicol.*, 2010, **26**, 143–152.
26 B. A. Messerle, A. Schäffer, M. Vasák, J. H. Kägi and K. Wüthrich, *J. Mol. Biol.*, 1992, **225**, 433–443.
27 H. Rupp and U. Weser, *Biochim. Biophys. Acta, Protein Struct.*, 1978, **533**, 209–226.
28 Z. Biron, S. Khare, A. O. Samson, Y. Hayek, F. Naider and J. Anglister, *Biochemistry*, 2002, **41**, 12687–12696.
29 M. Xu, L. M. Yang and Q. Q. Wang, *Chem.–Eur. J.*, 2012, **18**, 13989–13993.
30 M. Xu, X. W. Yan, Q. Q. Xie, L. M. Yang and Q. Q. Wang, *Anal. Chem.*, 2010, **82**, 1616–1620.
31 E. Hashimoto, T. B. Oyama, K. Oyama, Y. Nishimura, T. M. Oyama, T. Ueha-Ishibashi, Y. Okano and Y. Oyama, *Toxicol. in Vitro*, 2009, **23**, 1092–1099.
32 T. Kawanai, M. Satoh, K. Murao and Y. Oyama, *Toxicol. Lett.*, 2009, **191**, 231–235.

